*Desalination and Water Treatment*
www.deswater.com

doi: 10.5004/dwt.2021.26525

215 (2021) 328–346
March

# Application of artificial neural network, multiple linear regression, and response surface regression models in the estimation of monthly rainfall in Northern Cyprus

Youssef Kassem[a,b,*], Hüseyin Gökçekuş[b], Hüseyin Çamur[a], Engin Esenel[a]

[a]*Department of Mechanical Engineering, Engineering Faculty, Near East University, 99138 Nicosia (via Mersin 10, Turkey), Cyprus, Tel. +90 (392) 2236464; emails: yousseuf.kassem@neu.edu.tr/youssef.kassem1986@hotmail.com, (Y. Kassem) huseyin.camur@neu.edu.tr (H. Çamur), engin.esenel@neu.edu.tr (E. Esenel)*
[b]*Department of Civil Engineering, Civil and Environmental Engineering Faculty, Near East University, 99138 Nicosia (via Mersin 10, Turkey), Cyprus, email: huseyin.gokcekus@neu.edu.tr*

Received 10 April 2020; Accepted 29 August 2020

**ABSTRACT**

Forecasting the rainfall is one of the most important issues in the hydrological cycle. It is very challenging because is still unable to get an ideal model given its uncertain and unexpected variation. Therefore, the study reviewed previous scientific studied from 2000 to 2020 associated with predicting the rainfall in Northern Cyprus and worldwide using machine learning models or mathematical regressions. According to this review, it is evident that the response surface regression (RSR) model has not yet been considered in other studies about monthly rainfall prediction. Consequently, this paper is examined the performance of the RSR for monthly rainfall prediction and compared with the most prominent rainfall artificial model (feed-forward neural network) and multiple linear regression (MLR). In this work, geographical coordinates (latitude ($L$), longitude (Lo), and altitude (AL) of the location) and meteorological parameters (average temperature (AT), maximum temperature (Max$T$), minimum temperature (Min$T$), and relative humidity (Rh)) are considered as input variables for the models. Rainfall ($R$) is considered as an output variable for all models. The meteorological data were collected from seven meteorological stations distributed over Northern Cyprus for a short-term period (2011–2017). The coefficient of determination ($R^2$), root mean squared error (RMSE), Nash–Sutcliffe efficiency (NSE), and Willmott's index of agreement ($d$) were used to select the best predictive model. The results demonstrate that the developed ANN model is superior in predicting the value of monthly rainfall with reported values of 0.631, 33.404, 0.625, and 0.880 for the parameters of $R^2$, RMSE, NSE, and $d$, respectively. Additionally, the results indicate that the RSR model gave better represent the relationship between the geographical coordinates, meteorological parameters, and rainfall and produce a better prediction of the monthly rainfall compared to MLR.

*Keywords:* ANN; Northern Cyprus; MLR; Monthly rainfall; RSR

## 1. Introduction

Water availability and use depend on several factors including increased population, energy demand, and related environmental problems [1,2]. Water use is affected by both changes in land use and farming intensity in already cultivated lands. Moreover, according to Dercon and Christiaensen [3], Falco and Chavas [4], and Amare et al. [5], rainfall is considered a direct input for the production of crops, and rainfall variability can affect agricultural productivity, that is, rainfall could lead to a change in crops, which

* Corresponding author.

*Presented at the 2nd International Conference on the Environment Survival and Sustainability (ESS 2019), 7–11 October 2019, Nicosia, North Cyprus*

1944-3994/1944-3986 

could move production away from the planned production [6]. Therefore, sustainable agricultural production and climate change are interrelated processes [7]. Also, extreme weather events like warmer and drier conditions are associated with negative impacts on agricultural production [8]. Moreover, the growth of population, energy demand, and related environmental problems are the main factors affecting the availability of water [9,10]. Additionally, air temperature and rainfall are the essential factors that influence human activities such as urban water resources and agricultural production [11,12]. Also, rainfall is one of the most important variables of hydro-climate because of its significance for sustainable water management [13]. Thus, the accurate prediction of rainfall availability is beneficial for making management and can assist with the sustainable operation of water resource systems.

Northern Cyprus is likely to suffer increasing levels of climate change impacts because of its geographical location and weak human, economic, technological, and financial capacity to cope with the multiple impacts of these disruptions. Vulnerability to climate change is compounded by the over-dependence on climate-sensitive sectors. The land distribution of the northern part of Cyprus constitutes 56.7% of agricultural, 19.5% of forestry, 5.0% of the grassing area, 10.7% is covered by towns, villages, rivers, and reservoirs and nearly 8.2% is bare land with 87 km$^2$ of irrigable land [14]. Northern Cyprus has very limited water resources [15]. Rainfall is considered the main source of water in the Northern part of Cyprus. Generally, in Cyprus, more than two-thirds of the rainfall occurs between October and April [16].

### 1.1. Literature survey

In recent years, empirical approaches like artificial neural networks (ANN) and multiple linear regressions (MLR) have been used as powerful modeling tools in the estimation of rainfall data. ANNs have emerged as a powerful technique for modeling complex functional relationships. Moreover, the MLR is used to describe the relationship between two or more independent variables and one dependent variable. Many studies have utilized different techniques used for the prediction of hourly/daily/weakly/monthly rainfall in Northern Cyprus and worldwide. The key features of previous scientific studies are summarized in Table 1.

According to Table 1, it can be concluded that:

- Researchers have recently focused on modeling hourly/daily/weekly/monthly rainfall using artificial intelligence models.
- Researchers have utilized meteorological parameters such as minimum and maximum temperatures, wind speed, pressure, and relative humidity
- Few studies have used climatological parameters like sunshine duration and solar radiation as input data for the empirical model to estimate the hourly/daily/weekly/monthly rainfall.
- According to the authors' review, most works used machine learning models and mathematical regressions including least-squares support vector regression, linear regression, classical linear regression, cluster wise linear regression, and MLR for monthly/daily/hourly rainfall prediction.

### 1.2. Objective of the present work

Regarding the literature review, it reveals a clear lack of monthly rainfall prediction models in Northern Cyprus. According to the authors' review, most of the previous studies used machine learning models and mathematical regressions for monthly/daily/hourly rainfall prediction, but no studies have utilized the response surface regression model (RSR) for predicting the rainfall. To the best of our knowledge, there are no detailed studies in Northern Cyprus about estimating the monthly rainfall as a function of latitude, longitude, and altitude of its location and the number of the months at any point near the selected stations where there are no measurements. Therefore, the main aim of the present work is to predict the monthly rainfall for a short-term period as a function of geographical coordinates (latitude, longitude, and altitude of the location) and meteorological parameters (mean temperature, maximum temperature, minimum temperature, and relative humidity). These meteorological parameters are used as input variables for the proposed models based on the previous scientific studies in practically [63]. Gökçekuş et al. [63] concluded that temperature and relative humidity are considered important parameters that have a greater impact on the estimated rainfall. Also, they found that wind speed has a minimum effect on rainfall prediction. In this study, three empirical models, namely, feed-forward neural network, MLRs, and RSR model are developed to predict the monthly rainfall in Northern Cyprus. It is expected to investigate the interaction of geographical coordinates and selected meteorological parameters to monthly rainfall. Thus, contours are plotted to investigate interactive effects and optimize the parameters affecting the rainfall.

## 2. Materials and methods

### 2.1. Measurement data and description of climate data

The average monthly climate data for the 7 y period (2011–2017) are used. The data are recorded by the Meteorological Department located in at Lefkoşa in Northern Cyprus. The location and specific information of the selected stations are listed in Table 2 and illustrated in Fig. 1.

Moreover, the descriptive statistics of each station including mean, standard deviation ($\sigma$), variance coefficient ($C_v$), minimum (Min.), maximum (Max.), median (Med.), skewness ($S$), and kurtosis ($K$) are presented in Table 3. It is observed that the highest and lowest averaged temperatures are recorded in Girne and Boğaz with a value of 20.89°C and 13.34°C, respectively. In addition, for all stations, the averaged maximum temperature values are varied from 19.77, which obtained in Gazimağusa and 31.95, which recorded in Ercan during the investigation period (2001–2016). Additionally, it is found that the lowest minimum temperature value is recorded in Güzelyurt with a value of 7.58°C. The coefficients of variation of temperature are moderately high, ranging from 21.96 to 93.32 (Table 3). During the

Table 1
Summary of researchers' studies in the modeling of rainfall by artificial neural networks and mathematical model

| Reference | Location/country | Empirical approach | Input | Output |
|---|---|---|---|---|
| [17] | India | Artificial neural network | 1871–1960 monthly summer monsoon rainfall used as input | 1961–1994 monthly summer monsoon rainfall |
| [18] | Sokoto, Gusau, Katsina, Kano, Ngyry, Pokistum, Maiduguri, Zaria, Yelwa, Kaduna, Bauchi, Minna, Bida, Iiorin, Jos, Lbi, Yola, Lokoja and Makurdi, Nigeria | Least absolute deviation multiple regression | Sea level pressure at the Azores; SOI; monthly temperature for the study area; south and north Atlantic SST; NAO; monthly rainfall for stations in the Zairian basin; and monthly rainfall for stations in the study area. | Seasonal rainfall |
| [19] | Chandler, Oklahoma Mesonet | Artificial neural networks (ANNs), standard support, vector regression (SVR), least-squares support vector regression (LS-SVR), linear regression (LR), and a rain rate (RR) formula | 576 observations rainfall | Twenty-six observations rainfall |
| [20] | India | Feedforward artificial neural network model and multiple linear regression | Average monthly Indian rainfall (in mm) of June, July, and August, tropical-average (30 N–30 S) sea surface temperature anomalies (in °C) in June, July, and August and tropical rainfall indices in June, July, and August. | Summer-monsoon rainfall |
| [21] | Zhengzhou, Henan province | Generalized regression neural network, backpropagation neural network, and stepwise regression analysis | 75% of the annual rainfall data used as input data | 15% of the annual data used as output data |
| [22] | Ibadan, Nigeria | Statistical neural network and classical linear regression models | Temperature and relative humidity | Daily rainfall |
| [23] | Udupi district of Karnataka | Multilayered artificial neural network | Average monthly humidity and the average wind speed | Monthly rainfall |
| [24] | India | Genetic programming | Large-scale atmospheric circulation patterns from the tropical Pacific Ocean and those from the tropical Indian Ocean | Summer monsoon rainfall |
| [25] | Malaysia | Modified adaptive neuro-fuzzy inference system | 1997–2005 monthly rainfall used as input data | 2005–2008 monthly rainfall used as output data |
| [26] | Assam, India | Wavelet regression and artificial neural network | 60 y monthly rainfall data as input data | 40 y monthly rainfall data as output data |
| [27] | Northeast region of Thailand | Artificial neural network, Mamdani's fuzzy model, and ARMA models | 1981–1998 monthly rainfall used as input data | 1999–2001 monthly rainfall used as output data |

*(Continued)*

Table 1 Continued

| Reference | Location/country | Empirical approach | Input | Output |
|---|---|---|---|---|
| [28] | Malaysia | Artificial neural networks, adaptive neuro-fuzzy inference system, artificial neural networks-wavelet and adaptive neuro-fuzzy inference system-wavelet | 1997–2004 monthly rainfall used as input data | 2004–2008 monthly rainfall used as output data |
| [29] | Northwest of Iran | Feed-forward neural network and autocorrelation regressive integrated moving average | 27 y monthly rainfall used as input data | 12 y monthly rainfall used as output data |
| [30] | Queensland, Australia | Artificial neural networks | Rain, southern oscillation index, inter-decadal pacific oscillation, dipole mode index, maximum temperature and minimum temperature | Monthly rainfall |
| [31] | Australia | Artificial neural networks | Maximum temperature | Monthly rainfall |
| [32] | Delhi, India | Back-propagation algorithm, cascaded back-propagation, and layer recurrent artificial neural networks | Humidity and wind speed | Rainfall |
| [33] | Indonesia | Backpropagation neural network | 1986–2003 monthly rainfall used as input data | 2004–2008 monthly rainfall used as output data |
| [34] | Coonoor region, Nilgiri district | Backpropagation neural network and radial basis function neural network | 1979–2002 monthly rainfall data used as input | 2002–2006 monthly rainfall data used as output |
| [35] | Mashhad | Feed-forward perceptron network | Bi-monthly average of rainfall in 1 month ago, bi-monthly average of rainfall in two months ago, bi-monthly average of rainfall in three months ago, bi-monthly average of rainfall in four months ago, Bi-monthly average of rainfall in five months ago, long-term average of rainfall for the estimated month, last year rainfall for the estimated month | Current month rainfall |
| [36] | Oshodi, Lagos, Nigeria | Artificial neural network | 83% of monthly rainfall data used as input data | Monthly rainfall |
| [37] | India | Adaptive-neuro-fuzzy inference system | Wet day frequency, vapor pressure, maximum air temperature, minimum air temperature, and cloud cover | Monthly rainfall |
| [38] | Nigeria | Feed-forward backpropagation, a neural network, cascade-forward backpropagation, a neural network, distributed time-delay neural network, and nonlinear autoregressive exogenous network | Temperature and humidity | Daily rainfall |
| [39] | Ampel, Boyolali, Central Java | Artificial neural network | 2001–2013 monthly rainfall rate data used as input | 2014–2015 monthly rainfall rate |

| | | | | |
|---|---|---|---|---|
| [40] | Markurdi Ilorin, Lafia, Jos, Lokoja, Minna and Abuja, Nigeria | Artificial neural network | 80% of monthly rainfall data used as input data | Monthly rainfall |
| [41] | Victoria, Australia | Cluster wise linear regression | Maximum temperature, minimum temperature, evaporation, vapor, and solar radiation | Monthly rainfall |
| [42] | Japan | Multi-layer perceptron neural network (MLPNN) and radial basis function neural network | Atmospheric pressure, precipitation, temperature, vapor pressure, humidity, and wind speed | Total rainfall |
| [43] | Kunming, Lincang, and Mengzi, Yunnan Province, China. | Ensemble empirical mode decomposition – support vector machine – artificial neural network model | 1951–2007 daily rainfall used as input data | 2007–2015 daily rainfall used as output data |
| [44] | India | M5Tree model, multivariate adaptive regression spline, least-square support vector regression (LSSVR), a gene expressing programming (GEP), and artificial neural networks methods | Geographical information and periodicity | Rainfall |
| [45] | Pahang basin, Malaysia | Linear stochastic model – non-linear extreme learning machine method | 70% of monthly rainfall used as input data | 30% of monthly rainfall used as output data |
| [46] | Kano, Nigeria | Artificial neural network and linear regression | Southern oscillation index; nino1+2; nino3; nino3.4; nino4 | Monthly rainfall |
| [47] | Peninsular Malaysia | Clonal selection algorithm | Temperature, relative humidity | Monthly rainfall |
| [48] | India | Artificial neural network | Relative humidity, mean sea level pressure, maximum temperature, minimum temperature, average temperature, average wind speed, and wind direction | Daily summer monsoon rainfall |
| [49] | Bauchi, Nigeria | Multiple linear regression model and artificial neural network (ANN) | Monthly means of sea surface temperature, air temperature, specific humidity, relative humidity, and U-wind at a surface different pressure level | Seasonal rainfall |
| [50] | India | Conjugate gradient descent learning-based back-propagation artificial neural network | 1871–1971 average summer monsoon rainfall used as input data | 1972–1999 average summer monsoon rainfall used as output data |
| [51] | India | *K*-nearest neighbor (KNN), artificial neural network (ANN), and extreme learning machine (ELM) | 1871–2010 average summer monsoon rainfall used as input data | 2011–2016 average summer monsoon rainfall used as output data |
| [52] | Iran | Artificial neural networks (ANNs), learning-cellular automation (LCA), and novel hybrid method of ANN and CLA | Temperature, humidity, wind speed, and pressure | Daily rainfall |
| [53] | Ca Mau province, Vietnam | Multilayer feed-forward neural network, seasonal artificial neural network, ARIMA, and GA-SA models | 85% of monthly rainfall data used as input data | Monthly rainfall |

*(Continued)*

Table 1 Continued

| Reference | Location/country | Empirical approach | Input | Output |
|---|---|---|---|---|
| [54] | Benin City, Nigeria | Multiple linear regression and artificial neural network | The monthly temperature, wind speed, relative humidity, and vapor pressure | Seasonal Rainfall |
| [55] | Spain | Multilayer perceptron neural network | Average temperature, maximum temperature, minimum temperature, average wind speed, relative humidity, total rainfall, visibility, day, and month | Week-ahead rainfall |
| [56] | Western Australia | Multiple linear regression and artificial neural network | Lagged values of the oceanic climate drivers, El Niño southern oscillation, and Indian Ocean dipole | Seasonal rainfall |
| [57] | Taiwan | Hybrid gray model, autoregressive integrated moving average, and artificial neural network | 40 y annual maximum daily rainfall | 10 y annual maximum daily rainfall |
| [58] | Ikeja, Nigeria | Artificial neural network | Sea surface temperature (SST), U-wind at (surface, 700; 850; and 1,000), air temperature, specific humidity, ITD, and relative humidity. | Seasonal rainfall |
| [59] | Setif, Algeria | *K*-nearest weighted neighbours (WkNN) classification algorithm | 70% of the data used as input | Instantaneous rainfall |
| [60] | Peninsular Malaysia | Support vector machines (SVM), random forests (RF), and Bayesian artificial neural networks | Rainfall amount, average rainfall intensity, days with rainfall more than 95-th percentile rainfall, and dry days | Seasonal rainfall and rainfall extremes |
| [61] | Vietnam | Adaptive network-based fuzzy inference system optimized with particle swarm optimization, artificial neural networks and support vector machines | Maximum temperature, minimum temperature, wind speed, relative humidity, and solar radiation | Daily rainfall |
| [62] | Pakistan | Complete ensemble empirical mode decomposition (CEEMD) combined with random forest (RF) and kernel ridge regression (KRR) algorithms in designing a hybrid CEEMD-RF-KRR model | Rainfall data were collected from three stations | Monthly rainfall |
| [63] | Morphou, Northern Cyprus | Artificial neural networks | Minimum temperature, maximum temperature, average temperature, wind speed, global solar radiation, and sunshine duration | Monthly rainfall |
| [64] | Senegal | Multilayer perceptron-whale optimization algorithm (MLP-WOA) | 75% of the data used as input | Annual rainfall |
| [65] | Peninsular Malaysia | Convolutional neural network and wavelet transform | 80% of the data used as input | Monthly rainfall and daily rainfall |
| [66] | Northern Cyprus | Feed forward neural network, adaptive neural fuzzy inference system, and least square support vector machine | Previous time steps of the monthly rainfall | Current time step of monthly rainfall |

Table 2
Details of each location used in this study

| Location | Coordinates | | Altitude (m) | Characteristics of the Location |
|---|---|---|---|---|
| | Latitude (°N) | Longitude (°E) | | |
| Lefkoşa | 35° 10′ 12.9″ | 33° 21′ 31.32″ | 146 | Surrounded by building |
| Ercan | 35° 10′ 25.86″ | 33° 32′ 52.08″ | 105 | Airport |
| Girne | 35° 20′ 0.6″ | 33° 18′ 51.156″ | 7 | Coastal |
| Güzelyurt | 35° 12′ 3.528″ | 32° 59′ 26.808″ | 49 | Coastal |
| Gazimağusa | 35° 7′ 15.9924″ | 33° 56′ 15.1116″ | 7 | Coastal |
| Boğaz | 35° 18′ 58.428″ | 33° 57′ 12.636″ | 388 | Coastal |
| Alevkaya | 35° 16′ 59.52″ | 33° 32′ 0.6252″ | 623 | Coastal |


Fig. 1. Representative meteorological stations (squared: stations used in testing; circle: stations used in training).

investigation period, the Skewness values of all stations are varying, which depends on the station, that is, a positive value indicates that all distributions are right-skewed, while the negative value of skewness indicates that all distributions are left-skewed.

Moreover, for all stations, the mean rainfall values are varied from 21.68 to 45.5 mm as shown in Table 3, and mean rainfall over Northern Cyprus is about 225 mm. The coefficients of variation are moderately high, ranging from 77.79 to 106.98. In addition, the skewness values of all stations are positive indicating that all distributions are right-skewed.

Additionally, the variations of the monthly mean rainfall at each station for the years from 2011 to 2017 are illustrated in Fig. 2. It is observed that the monthly mean rainfall is varied from 606.7 to 2.03 mm and the general trend is that the mean rainfall decreases from May to September and then starts to increase afterward for the rest of the year. Furthermore, it is noticed that the maximum and minimum rainfall is recorded in winter and summer seasons at all studied stations, respectively. In comparison, it is found that Boğaz and Lefkoşa have the highest and lowest annual mean rainfall with a value of 50.38 and 23.95 mm, respectively.

Furthermore, the mean relative humidity in Northern Cyprus is approximately 63%. Based on the result, it is noticed that Boğaz has the lowest mean relative humidity and Güzelyurt has the highest mean relative humidity as shown in Table 3. In general, the mean climate data and standard deviation values suggest that there is good

Table 3
Statistical parameters of mean monthly climate data

| Parameter | Station | Mean | σ | $C_v$ | Min. | Med. | Max. | $S$ | $K$ |
|---|---|---|---|---|---|---|---|---|---|
| Rainfall (mm) | Girne | 37 | 38.7 | 104.67 | 0.1 | 24.2 | 105.7 | 0.86 | –0.77 |
| | Gazimağusa | 28.24 | 24.76 | 87.67 | 0 | 29.64 | 71.84 | 0.63 | –0.51 |
| | Güzelyurt | 24.47 | 19.03 | 77.79 | 1.5 | 23.24 | 57.27 | 0.57 | –0.43 |
| | Ercan | 24.83 | 19.98 | 80.49 | 0.04 | 26.11 | 65.64 | 0.62 | 0.04 |
| | Lefkoşa | 21.68 | 19.21 | 88.59 | 0.09 | 22.01 | 52.89 | 0.45 | –1.1 |
| | Boğaz | 45.5 | 48.6 | 106.98 | 0 | 28.8 | 133.2 | 0.88 | –0.67 |
| | Alevkaya | 43.7 | 38.5 | 88.16 | 0.1 | 41.3 | 127.7 | 0.79 | 0.49 |
| | Northern Cyprus | 225.4 | 201.3 | 89.3 | 2 | 199.2 | 606.7 | 0.69 | –0.43 |
| Average temperature (°C) | Girne | 20.89 | 6.05 | 28.96 | 13.1 | 20.19 | 29.57 | 0.18 | –1.56 |
| | Gazimağusa | 14.64 | 4.09 | 27.92 | 9.17 | 14.38 | 20.44 | 0.12 | –1.55 |
| | Güzelyurt | 18.77 | 6.45 | 34.38 | 10.47 | 18.53 | 27.8 | 0.13 | –1.59 |
| | Ercan | 19.65 | 7.16 | 36.46 | 10.2 | 19.55 | 29.59 | 0.09 | –1.6 |
| | Lefkoşa | 19.34 | 7.35 | 38.01 | 9.69 | 19.24 | 29.49 | 0.11 | –1.58 |
| | Boğaz | 13.34 | 4.57 | 34.22 | 7.07 | 13.28 | 19.57 | 0.05 | –1.59 |
| | Alevkaya | 16.8 | 6.64 | 39.54 | 7.99 | 16.61 | 26.19 | 0.13 | –1.53 |
| | Northern Cyprus | 19.17 | 6.61 | 34.5 | 10.51 | 18.85 | 28.39 | 0.12 | –1.58 |
| Maximum temperature (°C) | Girne | 28.53 | 6.44 | 22.55 | 19.77 | 28.07 | 37.61 | 0.09 | –1.51 |
| | Gazimağusa | 19.77 | 4.34 | 21.96 | 13.6 | 20.52 | 24.99 | –0.19 | –1.73 |
| | Güzelyurt | 31.95 | 7.42 | 23.21 | 20.13 | 33.73 | 41.39 | –0.27 | –1.4 |
| | Ercan | 31.47 | 7.9 | 25.12 | 19.16 | 33.21 | 40.57 | –0.3 | –1.55 |
| | Lefkoşa | 31.87 | 8.03 | 25.19 | 19.36 | 33.49 | 41.69 | –0.25 | –1.51 |
| | Boğaz | 20.11 | 5.12 | 25.47 | 12.34 | 20.7 | 26.3 | –0.16 | –1.58 |
| | Alevkaya | 27.47 | 7.62 | 27.75 | 15.79 | 28.89 | 36.9 | –0.21 | –1.55 |
| | Northern Cyprus | 29.74 | 7.32 | 24.63 | 18.62 | 30.95 | 38.86 | –0.19 | –1.54 |
| Minimum temperature (°C) | Girne | 14.59 | 5.62 | 38.5 | 5.69 | 15.02 | 22.63 | –0.12 | –1.21 |
| | Gazimağusa | 9.2 | 4.95 | 53.75 | 2.39 | 9.07 | 16.66 | 0.15 | –1.35 |
| | Güzelyurt | 7.58 | 6.74 | 88.93 | –0.8 | 7.19 | 17.51 | 0.19 | –1.52 |
| | Ercan | 9.09 | 7.31 | 80.4 | –0.11 | 8.44 | 19.7 | 0.18 | –1.55 |
| | Lefkoşa | 7.8 | 7.28 | 93.32 | –1.36 | 7.39 | 18.47 | 0.21 | –1.53 |
| | Boğaz | 7.62 | 4.66 | 61.1 | 0.87 | 7.15 | 14.63 | 0.07 | –1.36 |
| | Alevkaya | 8.25 | 6.42 | 77.84 | –0.5 | 7.48 | 17.66 | 0.11 | –1.45 |
| | Northern Cyprus | 9.89 | 6.6 | 66.79 | 0.99 | 9.03 | 19.46 | 0.19 | –1.52 |
| Relative humidity (%) | Girne | 60.885 | 3 | 4.93 | 56.371 | 61.25 | 64.757 | –0.19 | –1.71 |
| | Gazimağusa | 46.851 | 1.279 | 2.73 | 44.614 | 46.95 | 48.914 | –0.25 | –0.59 |
| | Güzelyurt | 67.75 | 4.75 | 7.01 | 63.09 | 66.65 | 76.11 | 0.79 | –0.93 |
| | Ercan | 60.26 | 7.82 | 12.98 | 50.67 | 57.97 | 73.23 | 0.51 | –1.11 |
| | Lefkoşa | 58.76 | 8.86 | 15.07 | 47.93 | 56.86 | 73.16 | 0.38 | –1.24 |
| | Boğaz | 44.67 | 4.64 | 10.4 | 38.44 | 42.79 | 52.4 | 0.42 | –0.95 |
| | Alevkaya | 66.9 | 8.69 | 12.99 | 53.69 | 65.53 | 80.27 | 0.15 | –0.97 |
| | Northern Cyprus | 63.25 | 5.83 | 9.22 | 55.7 | 62.52 | 72.81 | 0.44 | –1.08 |

σ, standard deviation; $C_v$, variance coefficient; Min., Minimum value of rainfall climate data; Max., Maximum value of rainfall climate data, Med., Median; $S$, Skewness, $K$, Kurtosis.

consistency in climate data behavior. In addition, Fig. 2 illustrates the mean monthly air temperature including maximum temperature, average temperature, and minimum temperature, respectively at selected stations. It is noticed that Gazimağusa and Lefkoşa have the lowest and highest mean maximum temperature as shown in Fig. 2. Also, it is noticed that Boğaz has the minimum average temperature compared to other stations. Moreover, it is found that the lowest and highest mean minimum temperature was recorded in January (≈1°C) and August (≈19.5°C). Besides, Fig. 2 highlights the monthly variation of mean relative humidity at seven stations and shows the monthly relative humidity of Northern Cyprus. For Girne, the monthly averaged relative humidity is varied from 68.50%

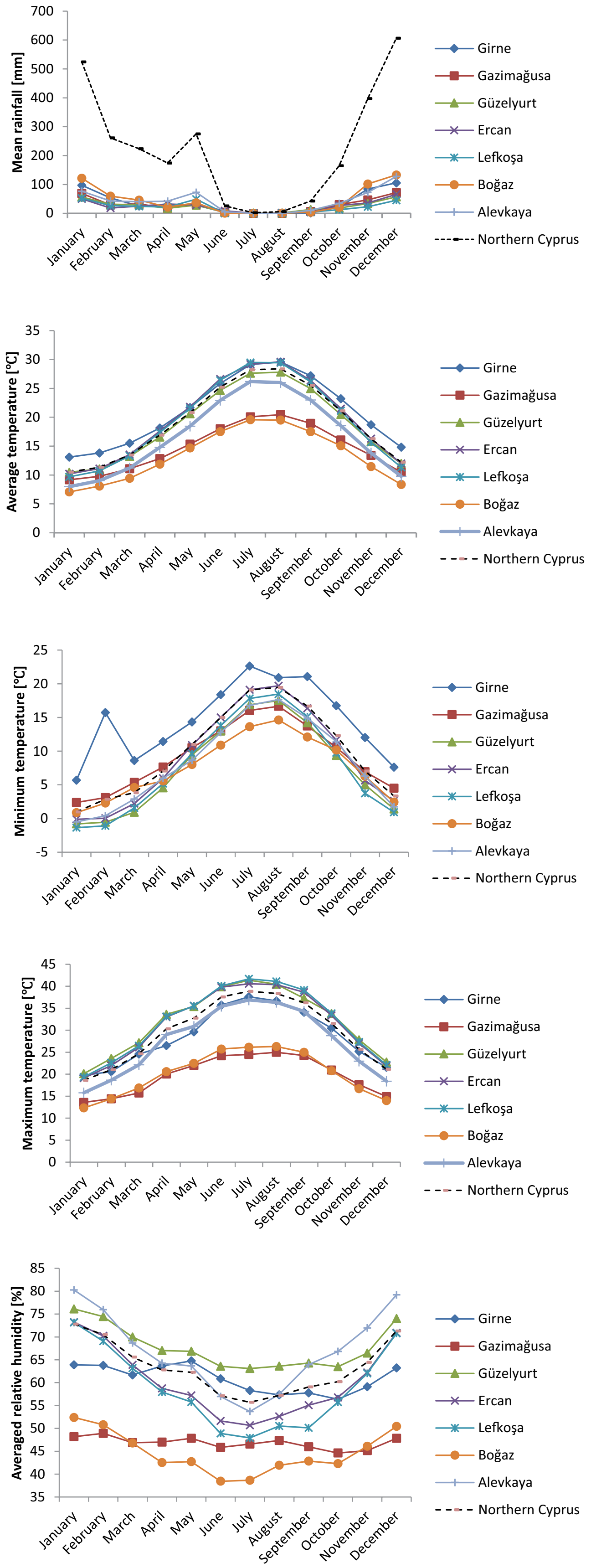


Fig. 2. Mean monthly of climate data.

to 44.30% with the minimum mean relative humidity recorded in October 2013. For Ercan, the monthly relative humidity falls gradually from January to June and begins to increase afterward. A similar trend is also observed at Güzelyurt, Lefkoşa, Boğaz, and Alevkaya. The minimum mean monthly relative humidity is occurred in October 2013 for all stations expected Lefkoşa and Alevkaya. As can be seen from Fig. 2, the lowest monthly relative humidity at Lefkoşa and Alevkaya is obtained in September 2014 and August 2013, respectively. In general, the annual relative humidity values are ranged between 58.828% and 67.90% with an average value of 63.20%.

### 2.2. Artificial neural network

The ANN is a powerful mathematical modeling tool, especially for complex systems. ANNs have long been used as an alternative methodology in different areas such as function approximation and so on. Many types of ANNs have been developed by scientific researchers such as which the feed-forward neural network is one of the most popular ANNs [67]. The node numbers in the input and output layers are estimated by the nature of the problem. Generally, the multilayer feed-forward neural network is widely used in solving engineering problems. It consists three layers, namely: input layer(s), hidden layer(s), and output layer(s). In addition, the number of these layers depends on the nature of the problem.

In this study, ANN method uses the altitude (AL), latitude (*L*), longitude (Lo), month number (Mn), average temperature (AT), minimum temperature (Min*T*), maximum temperature (Max*T*), and relative humidity (Rh) as input. In this work, TRAINLM is used as a training function that updates the weight and bias values of the neuron connections according to Levenberg–Marquardt (LM) optimization. The backpropagation algorithm is used as a learning algorithm and it is a gradient descent algorithm. The logistic-sigmoid (logsig) and tangent-sigmoid (tansig) are used as activation functions whose outputs lie between 0 and 1 and are defined as:

$$\text{logsig} = \frac{1}{1+e^{-x}} \tag{1}$$

$$\text{tansig} = \frac{e^{x}-e^{-x}}{e^{x}+e^{-x}} \tag{2}$$

The key step for developing an ANN is the training procedure, where the weights and biases are adjusted to minimize the difference between the output of the ANN and the actual value. In order to find the best performance for the ANN trained model, the mean squared error (MSE) is used. Fig. 3 presents the prediction processes used in the proposed MFFNN method. By trial and error, the optimum number of the nodes in the hidden layers, the most suitable transfer function, and the number of neurons are determined. In order to obtain the best performance results, various ANN models are designed. Fig. 4 shows the structure of the ANN model used in this study. Moreover, the logsig function and the tansig functions were used as the activation functions in the hidden layer and the output layer, respectively.

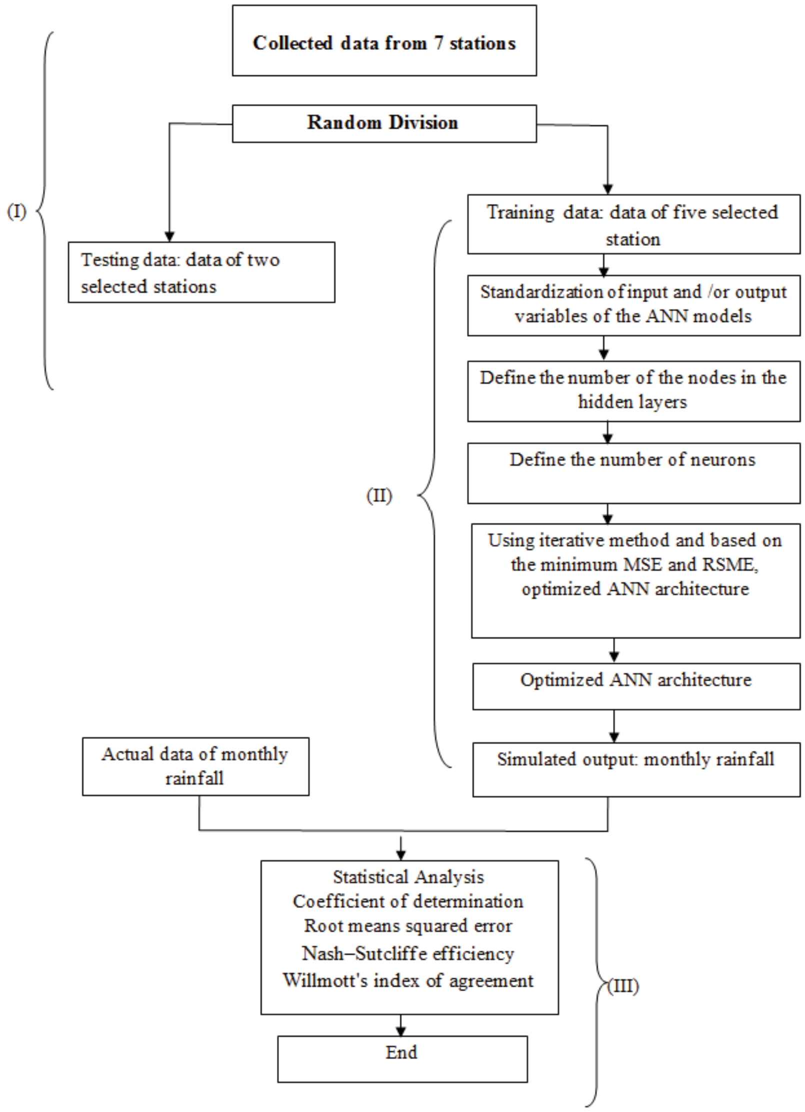


Fig. 3. Flowchart of the ANN-based method prediction procedure.

### 2.3. Multiple linear regressions

MLR is described as the relationship dependent ($y$) and independent variables ($x$). It can be expressed as:

$$y_i = \beta_0 + \beta_1 x_1 + \ldots + \beta_i x_i \qquad i = 1,2,\ldots,n \tag{3}$$

where $y_i$ denotes the dependent variable (rainfall) and $x_i$ where $i$ = 1,2,...,$n$ denotes the explanatory or independent variables and β is called the intercept. In order to evaluate the relationship between the dependent and independent variables, the Pearson correlation test is examined. SPSS was used for the regression and testing of the data.

### 2.4. RST model

The RSR model is a mathematical model that represents a simple description of a physical, chemical, or biological process. RSR has the advantage of reducing the number of measurements, which is sufficient to provide statistically acceptable results [68]. The RSR model of monthly rainfall is developed using a response surface methodology (RSM). This model is used to investigate the influence of interactive effects of the meteorological parameters and geographical coordinates on monthly rainfall, In the RSM method, the quantitative form of the relationship between the independent input variables and the desired output is expressed as follows:

$$R = f\left(\mathrm{AL}, L, \mathrm{Lo}, \mathrm{Mn}, \mathrm{AT}, \mathrm{Min}T, \mathrm{Max}T \text{ and } \mathrm{Rh}\right) \tag{4}$$

On the basis of the actual data, regression analysis was carried out by the following quadratic polynomial model:

$$R = \beta_0 + \sum_{i=1}^{n} \beta_i x_i + \sum_{i=1}^{n} \beta_{ii} x_i^2 + \sum_{i}^{n-1} \sum_{j=i+1}^{n} \beta_{ij} x_i x_j \tag{5}$$

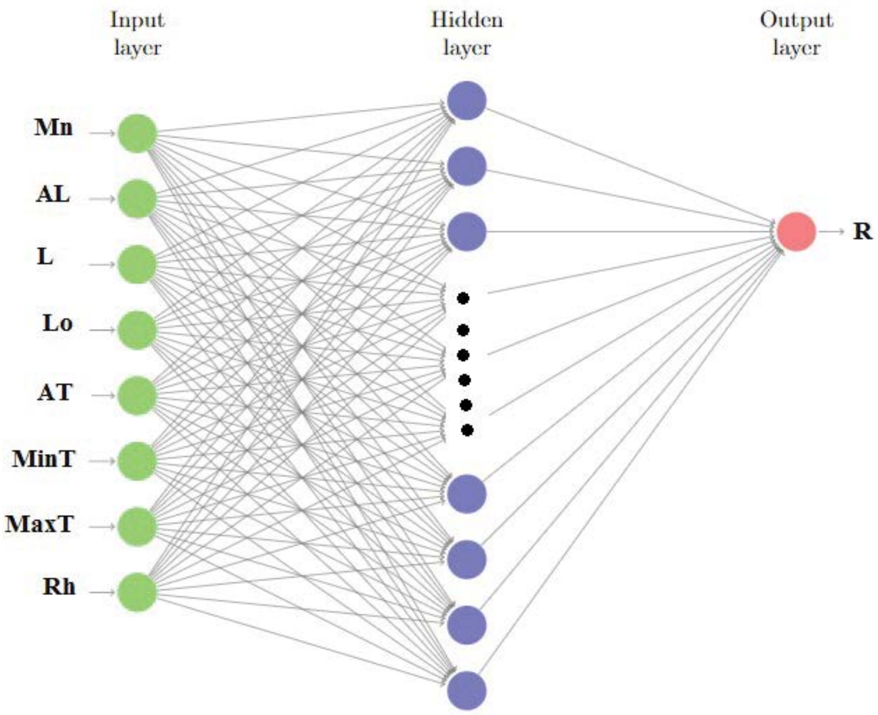


Fig. 4. Meteorological data used to estimate the structure of ANN.

where $\beta_0$ is the offset term; $\beta_i$ is the linear coefficient; the second-order coefficient and $\beta_{ij}$ is the interaction coefficient; $x_i$ and $x_j$ are the independent variables. The least-squares method was employed to ascertain the values of the model parameters and analysis of variance (ANOVA) was applied to establish their statistical significance at a confidence level of 95%. The Minitab statistical software 17 was used for the regression and graphical analysis of the data.

### 2.5. Model performance criteria

In general, the performance measures are utilized to select the "better" predictive model. The following statistical indicators are widely used to assess the predictive power of ANN and mathematical models [69,70].

*Coefficient of determination* ($R^2$):

$$R^2 = 1 - \frac{\sum_{i=1}^{n}\left(a_{a,i} - a_{p,i}\right)^2}{\sum_{i=1}^{n}\left(a_{p,i} - a_{a,\text{ave}}\right)^2} \quad (6)$$

*Mean squared error (MSE)*:

$$\text{MSE} = \frac{1}{n}\sum_{i=1}^{n}\left(a_{a,i} - a_{p,i}\right)^2 \quad (7)$$

*Root mean squared error (RMSE)*:

$$\text{RMSE} = \sqrt{\frac{1}{n}\sum_{i=1}^{n}\left(a_{a,i} - a_{p,i}\right)^2} \quad (8)$$

*Nash–Sutcliffe efficiency (NSE):*

$$\text{NSE} = 1 - \frac{\sum_{i-1}^{n}\left(a_{a,i} - a_{p,i}\right)^2}{\sum_{i-1}^{n}\left(a_{a,i} - a_{a,\text{ave}}\right)^2} \quad (9)$$

*Willmott's index of agreement* ($d$):

$$d = 1 - \frac{\sum_{i-1}^{n}\left(a_{a,i} - a_{p,i}\right)^2}{\sum_{i-1}^{n}\left(\left|a_{p,i} - a_{a,\text{ave}}\right| + \left|a_{a,i} - a_{a,\text{ave}}\right|\right)^2} \quad (10)$$

where $n$ is the number of data, $a_{p,i}$ is the predicted values, $a_{a,i}$ is the actual values, $a_{a,\text{ave}}$ is the average actual values, and $i$ is the number of input variables.

## 3. Results

### 3.1. ANN model

As mentioned previously, a feed-forward neural network was employed to predict the monthly rainfall for Northern Cyprus. In this study, the number of months, geographical coordinates (AL, $L$, and Lo), and meteorological variable parameters (AT, Min$T$, Max$T$, and Rh) were collected and used as input parameters and monthly rainfall as output parameters in the models. From the given data, the data of five selected station (Lefkoşa, Ercan, Girne, Güzelyurt, and Gazimağusa) were used for training and the rest of the data of two stations (Boğaz and Alevkaya) were utilized to test the model. A series of models are examined to estimate the optimum number of hidden layers (HL), the number of neurons (NN), and transfer function (TF) for the ANN model. It should be noted that the number of HLs and NNs in the ANN model was determined by utilizing trial and error approaches. Based on the value of MSE, it is found that 50 hidden layers and 15 neurons are selected as the best for ANN modeling (8:50:1) have the minimum MSE with a value of 0.0003512 compared to other models. Fig. 5 illustrates the *R*-squared for training data of rainfall data in Northern Cyprus. *R*-squared is used to evaluate the performance of artificial models. *R*-squared means the degree of the linear relationship between the observed and modeled values. The line is almost straight with a 45° angle and this proves the accuracy of the provided model. For the training phase, the $R^2$ value was found to be 0.9074 as shown in Fig. 5. The results obtained from the ANN models show that the use of ANN is enough to predict monthly rainfall.

### 3.2. MLR model

In this study, MLR method was developed to estimate the monthly rainfall (*R*) as a function of altitude (AL), latitude (*L*), longitude (Lo), month number (Mn), averaged temperature (AT), maximum temperature (Max*T*), minimum temperature (Min*T*), and relative humidity (Rh) with the climate data of 540 data for all stations in Northern Cyprus as shown in Eq. (11):

$$R = -1,543.670 - 0.296 \cdot \text{Mn} + 0.039 \cdot \text{AL} + 44.073 \cdot L + 1.127 \cdot \text{Lo} - 0.273 \cdot \text{AT} - 0.996 \cdot \text{Min}T - 1.377 \cdot \text{Max}T + 0.709 \cdot \text{Rh} \quad (11)$$

In the current study, the performances of the MLR were tested by Pearson product-moment correlation, which is used to investigate the relationship between the rainfall (*R*), geographical coordinates (AL, *L*, and Lo), and meteorological parameters (AT, Min*T*, Max*T*, and Rh) followed by a parametric method for normal distribution. According to Table 3, there are strong significant correlation coefficients between the temperatures and rainfall for all periods. Also, it is observed that there is a significant positive relationship between relative humidity and rainfall. The same results have been found by Gökçekuş et al. [63]. The authors concluded that temperature is considered as the most important parameter that has a greater impact on the estimated rainfall. It is found that wind speed has a minimum effect on rainfall prediction. According to Table 4, the *P*-value of Mn and Lo was 0.129 and 0.421, respectively, these values were greater than the pre-significant value of 0.05 thus, and they are not significant. Moreover, Fig. 6 illustrates the *R*-squared for training data of monthly rainfall data using MLR.

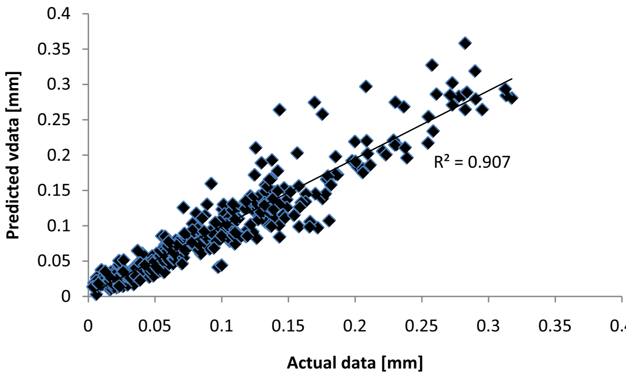


Fig. 5. Correlations between actual values and predicted value by optimum ANN model.

### 3.3. RSR models

The RSR model was used to study the response pattern and to determine the optimum combination of variables. The Minitab statistical software 17 was used for the regression and graphical analysis of the data. The time-series data were analyzed by the RSR using Eqs. (12)–(14) as shown below. The performances of the RSRs were tested by calculating the *R*-squared value. The high *R*-squared value indicates over-fit in the model. The *R*-squared value for rainfall data is shown in Fig. 7. It is found that the value of *R*-squared was 0.4074 for Eq. (12), 0.4459 for Eq. (13), and 0.4568 for Eq. (14). Also, it is observed that the full quadratic model has the highest value of *R*-squared compared to other models.

$$\begin{aligned} R = {} & 3,726,658 + 0.232 \cdot \text{Mn} + 0.118 \cdot \text{AL} - 212,882 \cdot L + 1,398\ \text{Lo} \\ & - 2.03 \cdot \text{AT} + 2.67 \cdot \text{Min}T - 8.21 \cdot \text{Max}T - 2.89 \cdot \text{Rh} \\ & - 0.0039 \cdot \text{Mn}^2 - 0.000141 \cdot \text{AL}^2 + 3,022 \cdot L^2 - 21.3 \cdot \text{Lo}^2 \\ & + 0.042 \cdot \text{AT}^2 - 0.1636 \cdot \text{Min}T^2 + 0.1188 \cdot \text{Max}T^2 \\ & + 0.0333 \cdot \text{Rh}^2 \end{aligned} \quad (12)$$

$$\begin{aligned} R = {} & -693,818 - 12.2 \cdot \text{Mn} + 17.7 \cdot \text{AL} + 19,676 \cdot L + 20,043 \cdot \text{Lo} \\ & - 299 \cdot \text{AT} + 122 \cdot \text{Min}T + 838 \cdot \text{Max}T + 57 \cdot \text{Rh} \\ & - 0.000647 \cdot \text{Mn} \cdot \text{AL} - 0.07 \cdot \text{Mn} \cdot L + 0.438 \cdot \text{Mn} \cdot \text{Lo} \\ & - 0.0722 \cdot \text{Mn} \cdot \text{AT} + 0.0327 \cdot \text{Mn} \cdot \text{Min}T + 0.0356 \cdot \text{Mn} \cdot \text{Max}T \\ & - 0.0001 \cdot \text{Mn} \cdot \text{Rh} - 0.85 \cdot \text{AL} \cdot L + 0.360 \cdot \text{AL} \cdot \text{Lo} \\ & + 0.00426 \cdot \text{AL} \cdot \text{AT} - 0.00833 \cdot \text{AL} \cdot \text{Min}T + 0.00664 \cdot \text{AL} \cdot \text{Max}T \\ & + 0.00147 \cdot \text{AL} \cdot \text{Rh} - 569 \cdot L \cdot \text{Lo} + 11.0 \cdot L \cdot \text{AT} - 4.8 \cdot L \cdot \text{Min}T \\ & - 23.2 \cdot L \cdot \text{Max}T - 1.10 \cdot L \cdot \text{Rh} - 1.92 \cdot \text{Lo} \cdot \text{AT} + 0.99 \cdot \text{Lo} \cdot \text{Min}T \\ & - 0.69 \cdot \text{Lo} \cdot \text{Max}T - 0.40 \cdot \text{Lo} \cdot \text{Rh} - 0.287 \cdot \text{AT} \cdot \text{Min}T \\ & - 0.193 \cdot \text{AT} \cdot \text{Max}T - 0.255 \cdot \text{AT} \cdot \text{Rh} + 0.352 \cdot \text{Min}T \cdot \text{Max}T \\ & + 0.119 \cdot \text{Min}T \cdot \text{Rh} - 0.017 \cdot \text{Max}T \cdot \text{Rh} \end{aligned} \quad (13)$$

$$\begin{aligned} R = {} & -3,832,459 + 1.4 \cdot \text{Mn} - 0.127 \cdot \text{AL} - 218,019 \cdot L - 224 \cdot \text{Lo} \\ & + 455 \cdot \text{AT} - 443 \cdot \text{Min}T + 614 \cdot \text{Min}T + 614 \cdot \text{Max}T + 42 \cdot \text{Rh} \\ & - 0.00268 \cdot \text{Mn}^2 - 0.000152\text{AL}^2 + 3.6 \cdot \text{Lo}^2 + 0.967 \cdot \text{AT}^2 \\ & - 0.009 \cdot \text{Min}T^2 + 0.327 \cdot \text{Max}T^2 + 0.0237 \cdot \text{Rh}^2 \\ & - 0.000572 \cdot \text{Mn} \cdot \text{AL} - 0.35 \cdot \text{Mn} \cdot L + 0.341 \cdot \text{Mn} \cdot \text{Lo} \\ & - 0.0859 \cdot \text{Mn} \cdot \text{AT} + 0.0428 \cdot \text{Mn} \cdot \text{Min}T + 0.0381 \cdot \text{Mn} \cdot \text{Max}T \\ & - 0.0027 \cdot \text{Mn} \cdot \text{Rh} + 0.0114 \cdot \text{Al} \cdot \text{AT} - 0.01282 \cdot \text{AL} \cdot \text{Min}T \\ & + 0.00395 \cdot \text{AL} \cdot \text{Max}T + 0.0136 \cdot \text{AL} \cdot \text{Rh} - 5.2 \cdot L \cdot \text{AT} \\ & + 8.1 \cdot L \cdot \text{Min}T + 19.1 \cdot L \cdot \text{Max}T - 0.98 \cdot L \cdot \text{Rh} - 7.18 \cdot \text{Lo} \cdot \text{AT} \\ & + 4.32 \cdot \text{Lo} \cdot \text{Min}T + 1.58 \cdot \text{Lo} \cdot \text{Max}T - 0.22 \cdot \text{Lo} \cdot \text{Rh} \\ & - 0.849 \cdot \text{AT} \cdot \text{Min}T - 1.339 \cdot \text{AT} \cdot \text{Max}T - 0.158 \cdot \text{AT} \cdot \text{Rh} \\ & + 0.822 \cdot \text{Min}T \cdot \text{Max}T + 0.093 \cdot \text{Min}T \cdot \text{Rh} + 0.006 \cdot \text{Max}T \cdot \text{Rh} \end{aligned} \quad (14)$$

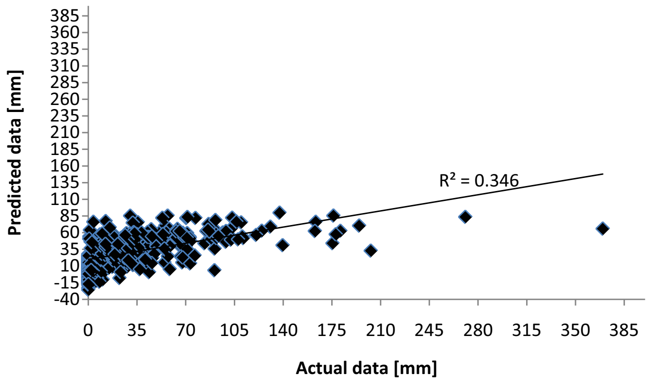


Fig. 6. Comparison between predicted data with actual data of rainfall using MLR.

Three-dimensional response surfaces were plotted based on the predicted model equation to investigate the interaction among the variables. The effect of climate variables on the rainfall is presented in Fig. 8. The contour plots of the rainfall indicate the interaction effects of parameters. In each contour graph, the interaction effect of the parameters was plotted. The contour areas help to explain how the viscosity and density vary with a change in the experimental conditions. The number written on each contour area indicates the rainfall in the specified conditions. These contour plots were demonstrated that the interaction effects of all parameters were considerable. In addition, the main effects plot for rainfall is presented in Fig. 9.

### *3.4. Comparison of empirical models for prediction rainfall*

As mentioned previously, to compare the performance of the models, the data of five selected station (Lefkoşa, Ercan, Girne, Güzelyurt, and Gazimağusa) were used for training and the rest of the data of two stations (Boğaz and Alevkaya). Furthermore, the *R*-squared, RMSE, NSE, and Willmott's index of agreement (*d*) are determined in order to select the best model for predicting monthly rainfall. *R*-squared is a measure of how well the regression line represents the data, while RMSE is a direct method for describing deviations. For high accuracy, *R*-squared must be close to 1.0, and the RMSE between the observed and predicted values must be as small as possible. Table 5 shows the results of the *R*-squared and RMSE values for all models. It is observed that the ANN model gave good predictions according to the *R*-squared and RMSE values for the testing data. Also, it is found that the RSR (Eq. (14)) has the highest value of *R*-squared and lowest value of RMSE for the testing data comparing to MLR, Eqs. (12) and (13). By comparing the computation results, the fitting precision of the ANN model is higher than those of other models, where the highest $R^2$ and least RMSE are 0.631 and 33.404, respectively.

Moreover, the NSE is generally similar to the $R^2$ measure for goodness-of-fit. A value of NSC = 1 indicates perfectly good forecasting accuracy; NSE = 0 when a forecast is no better than using the mean of the observed data; and NSE has negative values when a forecast is less accurate than the reference forecast. Thus, it is found that the NSE value for the ANN model and RSR models show that the models are satisfactory but the MLR is not satisfactory.

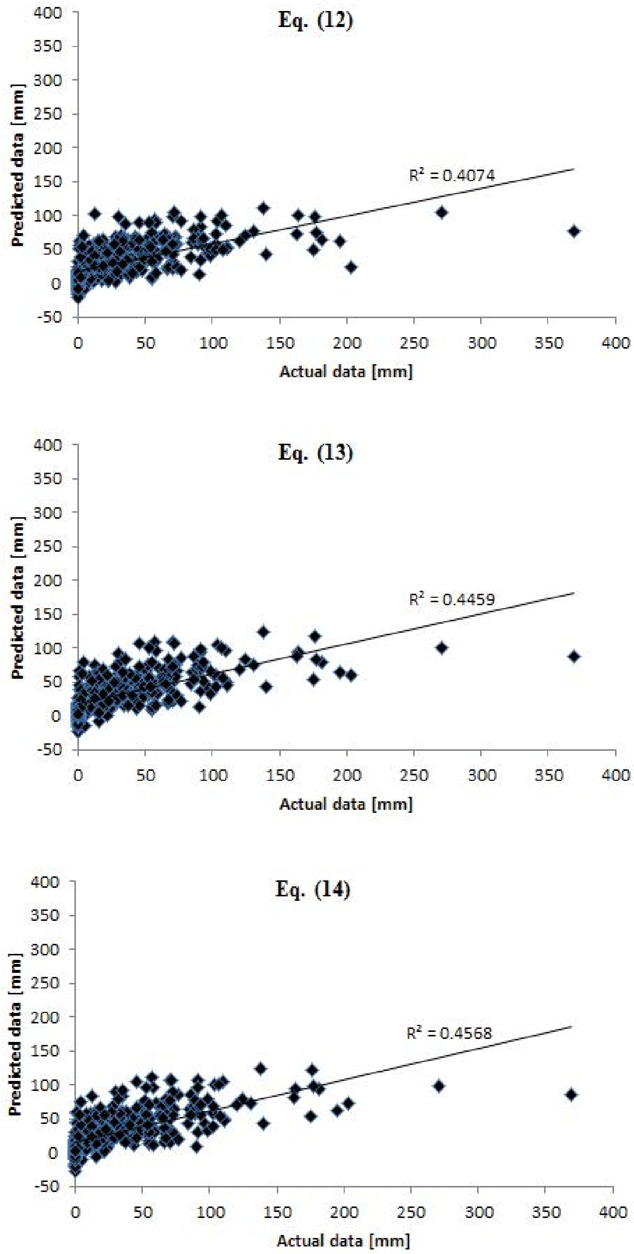


Fig. 7. Comparison between predicted data with actual data of rainfall using RSR.

Additionally, the NSE value for the ANN model is 0.625, which indicates that it is acceptable as shown in Table 5.

Furthermore, the performance of the predictive models is evaluated using Willmott's index of agreement (*d*). Willmott's index of agreement (*d*) is a standard measure to determine the error degree of the model. As shown in Table 5, it is found that the ANN model is the best and that the other models of monthly rainfall are also acceptable with the exception of MLR.

Moreover, Fig. 10 shows the comparison of the estimated and observed values of the mean monthly rainfall for all models.

Table 4
Correlations and $P$-value

| | | Mn | AL | $L$ | Lo | AT | Min$T$ | Max$T$ | Rh | $R$ |
|---|---|---|---|---|---|---|---|---|---|---|
| Mn | Pearson correlation | 1 | | | | | | | | |
| | Significance (2-tailed) | | | | | | | | | |
| AL | Pearson correlation | 0.883[b] | 1 | | | | | | | |
| | Significance (2-tailed) | 0 | | | | | | | | |
| $L$ | Pearson correlation | 0.083 | 0.383[b] | 1 | | | | | | |
| | Significance (2-tailed) | 0.084 | 0 | | | | | | | |
| Lo | Pearson correlation | 0.257[b] | 0.291[b] | –0.062 | 1 | | | | | |
| | Significance (2-tailed) | 0 | 0 | 0.199 | | | | | | |
| AT | Pearson correlation | –0.155[b] | –0.173[b] | –0.032 | 0 | 1 | | | | |
| | Significance (2-tailed) | 0.001 | 0 | 0.502 | 0.999 | | | | | |
| Min$T$ | Pearson correlation | –0.195[b] | –0.125[b] | 0.111[a] | 0.126[b] | 0.952[b] | 1 | | | |
| | Significance (2-tailed) | 0 | 0.01 | 0.021 | 0.009 | 0 | | | | |
| Max$T$ | Pearson correlation | –0.018 | –0.120[a] | –0.132[b] | –0.178[b] | 0.917[b] | 0.794[b] | 1 | | |
| | Significance (2-tailed) | 0.706 | 0.013 | 0.006 | 0 | 0 | 0 | | | |
| Rh | Pearson correlation | 0.055 | 0.151[b] | 0.01 | –0.024 | –0.668[b] | –0.567[b] | –0.666[b] | 1 | |
| | Significance (2-tailed) | 0.258 | 0.002 | 0.841 | 0.622 | 0 | 0 | 0 | | |
| $R$ | Pearson correlation | 0.073 | 0.170[b] | 0.162[b] | 0.039 | –0.543[b] | –0.475[b] | –0.555[b] | 0.460[b] | 1 |
| | Significance (2-tailed) | 0.129 | 0 | 0.001 | 0.421 | 0 | 0 | 0 | 0 | |

[a]Correlation is significant at the 0.05 level (2-tailed).
[b]Correlation is significant at the 0.01 level (2-tailed).

## 4. Discussions

The findings of this study are important for agricultural production and other socio-economic activities, which are directly concerned with the rainfed agricultural system. The rainfed agricultural system is significantly impacted by rainfall in addition to anthropogenic forces. Based on the analysis, it is found that the mean values of monthly rainfall were within the range of 2.0–606.7 mm in Northern Cyprus during the investigation period. In addition, it is observed that the amount of rainfall shows a strong positive correlation with temperatures (mean temperature, minimum temperature, and maximum temperature) and relative humidity. Developing an accurate model to capture the dynamic connection between rainfall and weather parameters remains a problematic task for engineers. In this study, the proposed model (RSR) is used to predict monthly rainfall in northern Cyprus and compared with two popular models (ANN and MLR) in order to obtain more accurate results when predicting the monthly rainfall. Based on the findings, the lowest value RMSE of 33.404 and the highest $R$-squared of 0.631 are provided by the ANN model followed by RSR (full quadratic model, Eq. (14)) with a value of RMSE of 41.657 and $R$-squared of 0.411 (Table 4). Therefore, the ANN and full quadratic model, Eq. (14), models can better represent the relationship between the meteorological parameters, geographical coordinates, and rainfall and produce a better prediction of the monthly rainfall. To ensure the accuracy of the proposed model, the performance results of the developed models are compared to previous scientific studies, which used meteorological parameters as input for the predictive model to predict the monthly rainfall. For instance, Abbot and Marohasy [30] evaluated the accuracy of ANN, climatology, and the predictive ocean atmosphere model with different combinations of input parameters to estimate the monthly rainfall in Queensland, Australia. The results found that RSME values were varied between 38.8 and 137.7 and the ANN model can give a better forecast than climatology even when only using the binary inputs (Max$T$, Min$T$, southern oscillation index, inter-decadal pacific oscillation, and dipole mode index). Ewona et al. [36] estimated the monthly rainfall for three weather measuring stations spread across using the ANN model. The results showed that correlation coefficients were within the range of 0.20–0.80. Bagirov et al. [41] proposed the clusterwise linear regression technique for the prediction of monthly rainfall and compared it with MLR, ANNs, and the support vector machines. The results indicated that the proposed algorithm outperformed other methods in most locations based on RMSE, which ranged from 19.7 to 39.3. Gökçekuş et al. [63] developed 25 ANN models to predict the monthly rainfall by varying the meteorological parameters. The results showed that ANN-17 with the combination of ($T_{min}$, $T_{max}$, SD, and GSR) had the maximum $R$-squared (0.6488) compared to the other models. Additionally, based on RMSE, they found that ANN-23 with a combination of ($T_{min}$, $T_{max}$, $T_{av}$, $W$, and SD) gave the lowest value of RMSE (0.1259) and was the best fit for predicting the monthly rainfall. Anh et al. [53] introduced novel hybrid models for monthly rainfall prediction, which were combined of two pre-processing methods (seasonal decomposition and discrete wavelet transform) and two feed-forward neural networks (ANN and seasonal ANN). The results showed that the model with the combination of Meyer wavelet and seasonal ANN provided the lowest RMSE and highest $R$-squared with values

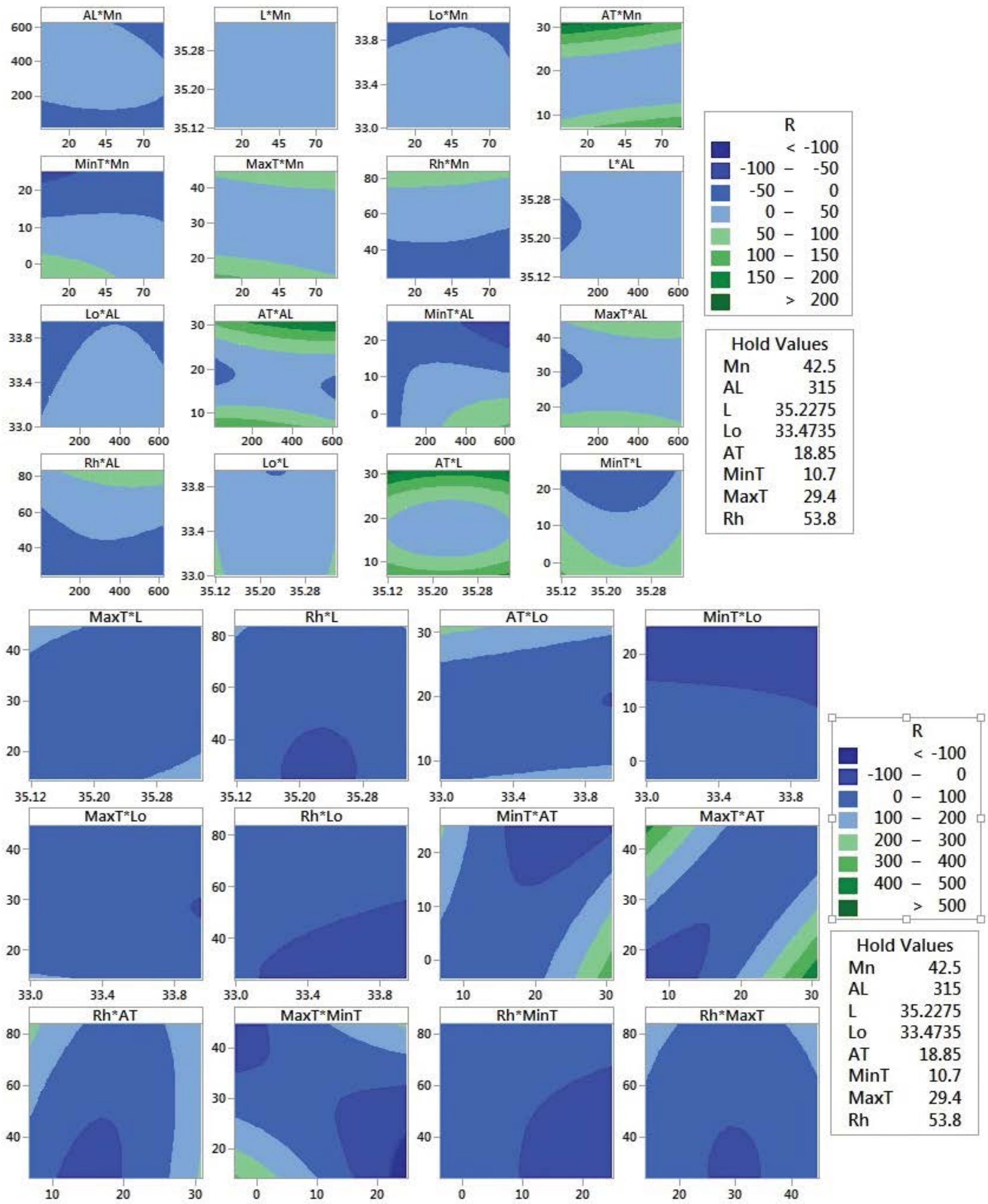


Fig. 8. Contour plots of rainfall data.

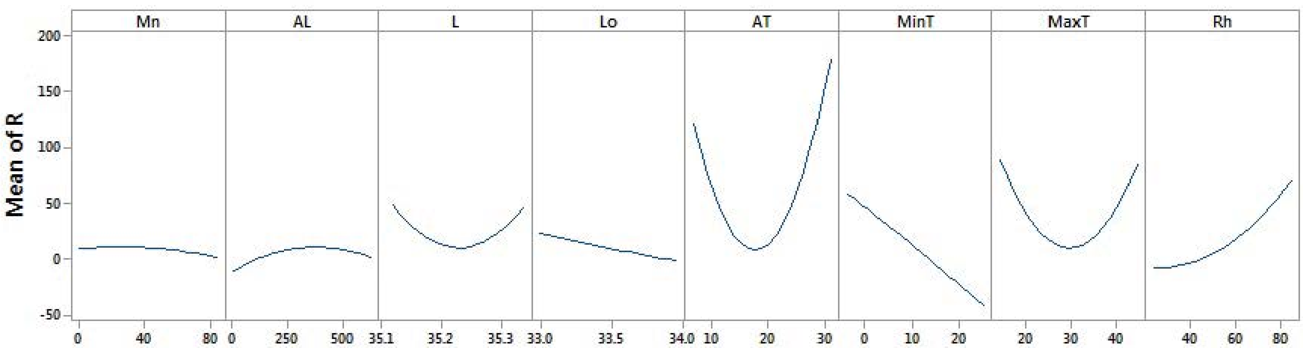


Fig. 9. Main effects plot for mean rainfall data.

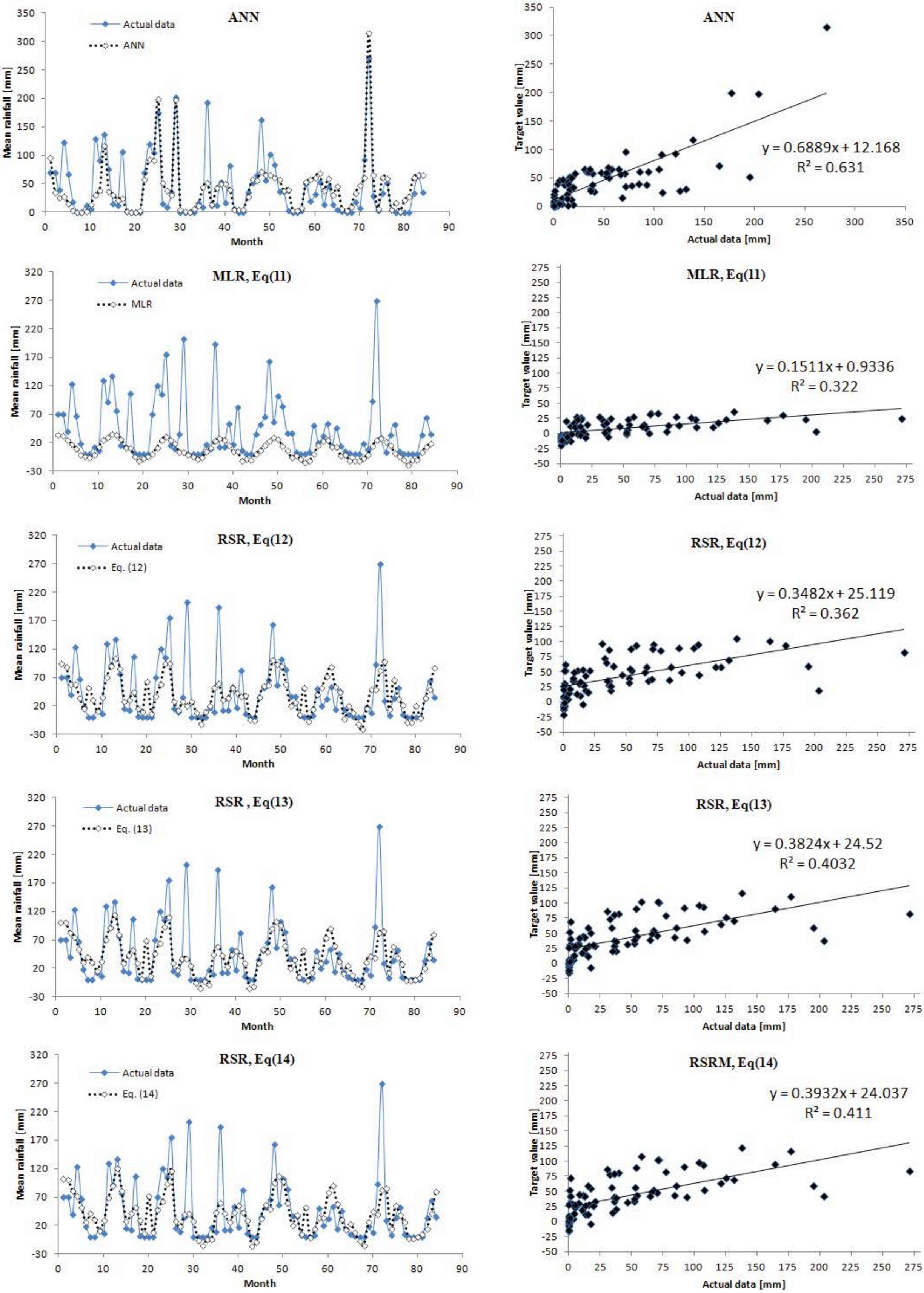


Fig. 10. Comparison of the predicted and observed values of the mean monthly rainfall for all models.

Table 5
Performance evaluation of the proposed models

| Performance criteria | ANN | MLR Eq. (11) | RSR | | |
|---|---|---|---|---|---|
| | | | Eq. (12) | Eq. (13) | Eq. (14) |
| *R*-squared | 0.631 | 0.322 | 0.362 | 0.403 | 0.411 |
| RMSE | 33.404 | 59.954 | 43.706 | 42.248 | 41.957 |
| NSE | 0.625 | –0.208 | 0.358 | 0.400 | 0.408 |
| *d* | 0.880 | 0.334 | 0.685 | 0.718 | 0.727 |

NSE: Nash–Sutcliffe efficiency; *d*: Willmott's index of agreement.

of 12.105 and 0.9973, respectively. Also, among the models, it was found that ARIMA model had the lowest value of *R*-squared (0.7628) and the highest value of RMSE (108.07). Consequently, it was concluded that the proposed models (ANN and RSR) could satisfactorily simulate non-stationary and non-linear time series-related problems such as rainfall prediction, but ANN provided the most accurate prediction for monthly rainfall.

## 5. Conclusions

Rainfall is one of the most important variables affecting the hydraulic behavior. Also, rainfall is considered the hardest weather variable to predict, and its cause-effect relationships often cannot be expressed in simple or complex mathematical forms. Therefore, the main objective of the study was to examine the application RSR model for monthly rainfall prediction in northern Cyprus. Also, this study was developed and compared two models namely, ANNs and MLR models with RSR for the prediction of monthly rainfall. For this, the number of months, geographical coordinates (AL, *L*, and Lo), and meteorological variable parameters (AT, Min*T*, Max*T*, and Rh) were collected and used as input parameters and monthly rainfall as output parameters in the models. Validation of the developed models was achieved using various quality assessment criteria such as coefficient of determination ($R^2$), RMSE, Nash–Sutcliffe efficiency (NSE), and Willmott's index of agreement (*d*). The results presented in this paper demonstrated that the ANN model was found to be the best method for predicting rainfall and was more precise compared to RSR and MLR models. Additionally, it is found that the RSR model is a good alternative model for predicting the monthly rainfall compared to the MLR model.

## Acknowledgments

The authors would like to thank the Faculty of Civil and Environmental Engineering especially the Civil Engineering Department and Engineering Faculty mainly Mechanical Engineering Department at Near East University for their support and encouragement.

## References

[1] Y. Kassem, H. Gökçekuş, Water resources and rainfall distribution function: a case study in Lebanon, Desal. Water Treat., 177 (2020) 306–321.
[2] S. Kundu, D. Khare, A. Mondal, Future changes in rainfall, temperature, and reference evapotranspiration in central India by least square support vector machine, Geosci. Front., 8 (2017) 583–596.
[3] S. Dercon, L. Christiaensen, Consumption risk, technology adoption and poverty traps: evidence from Ethiopia, SSRN Electron. J., 4257 (2008) 1–41.
[4] S.D. Falco, J.P. Chavas, On crop biodiversity, risk exposure, and food security in the highlands of Ethiopia, Am. J. Agric. Econ., 91 (2009), 599–611.
[5] M. Amare, N.D. Jensen, B. Shiferaw, J.D. Cissé, Rainfall shocks and agricultural productivity: implication for rural household consumption, Agric. Syst., 166 (2018) 79–89.
[6] O.E. Olayide, O.T. Alabi, Between rainfall and food poverty: assessing vulnerability to climate change in an agricultural economy, J. Cleaner Prod., 198 (2018) 1–10.
[7] O.E. Olayide, I.K. Tetteh, L. Popoola, Differential impacts of rainfall and irrigation on agricultural production in Nigeria: any lessons for climate-smart agriculture?, Agric. Water Manage, 178 (2016) 30–36.
[8] A.F. Ribeiro, A. Russo, C.M. Gouveia, P. Páscoa, Copula-based agricultural drought risk of rainfed cropping systems, Agric. Water Manage., 223 (2019) 105689, doi: 10.1016/j.agwat.2019.105689.
[9] M. Song, R. Wang, X. Zeng, Water resources utilization efficiency and influence factors under environmental restrictions, J. Cleaner Prod., 184 (2018) 611–621.
[10] S. Kundu, D. Khare, A. Mondal, Future changes in rainfall, temperature and reference evapotranspiration in the central India by least square support vector machine, Geosci. Front., 8 (2017) 583–596.
[11] N. Seino, T. Aoyagi, H. Tsuguti, Numerical simulation of urban impact on precipitation in Tokyo: how does urban temperature rise affect precipitation?, Urban Clim., 23 (2018) 8–35.
[12] T. Iizumi, N. Ramankutty, How do weather and climate influence cropping area and intensity?, Global Food Secur., 4 (2015) 46–50.
[13] R.K. Chowdhury, S. Beecham, Influence of SOI, DMI and niño3.4 on south Australian rainfall, Stochastic Environ. Res. Risk Assess., 27 (2013) 1909–1920.
[14] O.P. Agboola, F. Egelioglu, Water scarcity in north Cyprus and solar desalination research: a review, Desal. Water Treat., 43 (2012) 29–42.
[15] G. Elkiran, F. Aslanova, S. Hiziroglu, Effluent water reuse possibilities in northern Cyprus, Water, 11 (2019) 1–13, doi: 10.3390/w11020191.
[16] A. Sofroniou, S. Bishop, Water scarcity in cyprus: a review and call for integrated policy, Water, 6 (2014) 2898–2928.
[17] A.K. Sahai, M.K. Soman, V. Satyan, All India summer monsoon rainfall prediction using an artificial neural network, Clim. Dyn., 16 (2000) 291–302.
[18] O.A. Nnaji, Forecasting seasonal rainfall for agricultural decision-making in northern Nigeria, Agric. For. Meteorol., 107 (2001) 193–205.
[19] T.B. Trafalis, B. Santosa, M.B. Richman, Learning networks in rainfall estimation, Comput. Manage. Sci., 2 (2005) 229–251.
[20] S. Chattopadhyay, Feed forward artificial neural network model to predict the average summer-monsoon rainfall in India, Acta Geophys., 55 (2007) 369–382.

[21] Z.L. Wang, H.H. Sheng, Rainfall Prediction Using Generalized Regression Neural Network: Case Study Zhengzhou, 2010 International Conference on Computational and Information Sciences, Zhengzhou, 2010.

[22] C.G. Udomboso, G.N. Amahia, Comparative analysis of rainfall prediction using statistical neural network and classical linear regression model, J. Mod. Math. Stat., 5 (2011) 66–70.

[23] K. Abhishek, A. Kumar, R. Ranjan, S. Kumar, A Rainfall Prediction Model Using Artificial Neural Network, 2012 IEEE Control and System Graduate Research Colloquium, Shah Alam, Selangor, Malaysia, 2012.

[24] S.S. Kashid, R. Maity, Prediction of monthly rainfall on homogeneous monsoon regions of India based on large scale circulation patterns using genetic programming, J. Hydrol., 454 (2012) 26–41.

[25] S.A. Akrami, A. El-Shafie, O. Jaafar, Improving rainfall forecasting efficiency using modified adaptive neuro-fuzzy inference system (MANFIS), Water Resour. Manage., 27 (2013) 3507–3523.

[26] M.K. Goyal, Monthly rainfall prediction using wavelet regression and neural network: an analysis of 1901–2002 data, Assam, India, Theor. Appl. Climatol., 118 (2013) 25–34.

[27] J. Kajornrit, K.W. Wong, C.C. Fung, Y.S. Ong, An Integrated Intelligent Technique for Monthly Rainfall Time Series Prediction, 2014 IEEE International Conference on Fuzzy Systems (FUZZ-IEEE), Beijing, China, 2014.

[28] S.A. Akrami, V. Nourani, S.J.S. Hakim, Development of nonlinear model based on wavelet-ANFIS for rainfall forecasting at Klang Gates Dam, Water Resour. Manage., 28 (2014) 2999–3018.

[29] J. Farajzadeh, A.F. Fard, S. Lotfi, Modeling of monthly rainfall and runoff of Urmia lake basin using "feed-forward neural network" and "time series analysis" model, Water Resour. Ind., 7–8 (2014) 38–48.

[30] J. Abbot, J. Marohasy, Input selection and optimization for monthly rainfall forecasting in Queensland, Australia, using artificial neural networks, Atmos Res., 138 (2014) 166–178.

[31] J. Marohasy, J. Abbot, Assessing the quality of eight different maximum temperature time series as inputs when using artificial neural networks to forecast monthly rainfall at Cape Otway, Australia, Atmos. Res., 166 (2015) 141–149.

[32] A. Chaturvedi, Rainfall prediction using back-propagation feed forward network, Int. J. Comput. Appl., 119 (2015) 1–5.

[33] Mislan, Haviluddin, S. Hardwinarto, Sumaryono, M. Aipassa, Rainfall monthly prediction based on artificial neural network: a case study in Tenggarong Station, East Kalimantan – Indonesia, Procedia Comput. Sci., 59 (2015) 142–151.

[34] A. Kumar, N. Tyagi, Comparative Analysis of Backpropagation and RBF Neural Network on Monthly Rainfall Prediction, 2016 International Conference on Inventive Computation Technologies (ICICT), Coimbatore, India, 2016.

[35] N. Khalili, S.R. Khodashenas, K. Davary, M.M. Baygi, F. Karimaldini, Prediction of rainfall using artificial neural networks for synoptic station of Mashhad: a case study, Arabian J. Geosci., 9 (2016), doi: 10.1007/s12517-016-2633-1.

[36] I.O. Ewona, J.E. Osang, U.I. Uquetan, E.O. Inah, S.O. Udo, Rainfall prediction in Nigeria using artificial neural networks, Int. J. Sci. Eng. Res., 7 (2016) 1157–1169.

[37] R. Hashim, C. Roy, S. Motamedi, S. Shamshirband, D. Petković, M. Gocic, S.C. Lee, Selection of meteorological parameters affecting rainfall estimation using neuro-fuzzy computing methodology, Atmos. Res., 171 (2016) 21–30.

[38] S.R. Devi, P. Arulmozhivarman, C. Venkatesh, P. Agarwal, Performance comparison of artificial neural network models for daily rainfall prediction, Int. J. Autom. Comput., 13 (2016) 417–427.

[39] H.D. Purnomo, K.D. Hartomo, S.Y.J. Prasetyo, Artificial neural network for monthly rainfall rate prediction, IOP Conf. Ser.: Mater. Sci. Eng., 180 (2017) 1–9, doi: 10.1088/1757-899X/180/1/012057.

[40] T.S. Abdulkadir, A.W. Salami, A.S. Aremu, A.M. Ayanshola, D.O. Oyejobi, Assessment of neural networks performance in modeling rainfall amounts, J. Res. For. Wildl. Environ., 9 (2017) 12–22.

[41] A.M. Bagirov, A. Mahmood, A. Barton, Prediction of monthly rainfall in Victoria, Australia: clusterwise linear regression approach, Atmos. Res., 188 (2017) 20–29.

[42] T. Kashiwao, K. Nakayama, S. Ando, K. Ikeda, M. Lee, A. Bahadori, A neural network-based local rainfall prediction system using meteorological data on the internet: a case study using data from the Japan meteorological agency, Appl. Soft Comput., 56 (2017) 317–330.

[43] Y. Xiang, L. Gou, L. He, S. Xia, W. Wang, A SVR–ANN combined model based on ensemble EMD for rainfall prediction, Appl. Soft Comput., 73 (2018) 874–883.

[44] R. Mirabbasi, O. Kisi, H. Sanikhani, S.G. Meshram, Monthly long-term rainfall estimation in Central India using M5Tree, MARS, LSSVR, ANN and GEP models, Neural Comput. Appl., 31 (2018) 6843–6862.

[45] M. Zeynoddin, H. Bonakdari, A. Azari, I. Ebtehaj, B. Gharabaghi, H.R. Madavar, Novel hybrid linear stochastic with non-linear extreme learning machine methods for forecasting monthly rainfall a tropical climate, J. Environ. Manage., 222 (2018) 190–206.

[46] A. Bello, M. Mamman, Monthly rainfall prediction using artificial neural network: a case study of Kano, Nigeria, Environ. Earth Sci. Res. J., 5 (2018) 37–41.

[47] N. Rodi, M. Malek, A. Ismail, Monthly rainfall prediction model of peninsular Malaysia using clonal selection algorithm, Int. J. Eng. Technol., 7 (2018) 182–185.

[48] S. Hudnurkar, N. Rayavarapu, Performance of Artificial Neural Network in Nowcasting Summer Monsoon Rainfall: A case Study, IEEE Punecon, Pune, 2018.

[49] E.E. Peter, E.E. Precious, Skill comparison of multiple-linear regression model and artificial neural network model in seasonal rainfall prediction-north east Nigeria, Asian Res. J. Math., 11 (2018) 1–10.

[50] S. Chattopadhyay, G. Chattopadhyay, Conjugate gradient descent learned ANN for Indian summer monsoon rainfall and efficiency assessment through Shannon-Fano coding, J. Atmos. Sol. Terr. Phys., 179 (2018) 202–205.

[51] Y. Dash, S.K. Mishra, B.K. Panigrahi, Rainfall prediction for the Kerala state of India using artificial intelligence approaches, Comput. Electr. Eng., 70 (2018) 66–73.

[52] R. Mohammadpour, Z. Asaie, M.R. Shojaeian, M. Sadeghzadeh, A hybrid of ANN and CLA to predict rainfall, Arabian J. Geosci., 11 (2018), doi: 10.1007/s12517-018-3804-z.

[53] D.T. Anh, T.D. Dang, S.P. Van, Improved rainfall prediction using combined pre-processing methods and feed-forward neural networks, J, 2 (2019) 65–83.

[54] I.R. Ilaboya, O.E. Igbinedion, Performance of multiple linear regression (MLR) and artificial neural network (ANN) for the prediction of monthly maximum rainfall in Benin City, Nigeria, Int. J. Eng. Sci. Appl., 3 (2019) 21–37.

[55] L.C.P. Velasco, R.P. Serquiña, M.S.A. Zamad, B.F. Juanico, J.C. Lomocso, Week-ahead rainfall forecasting using multilayer perceptron neural network, Procedia Comput. Sci., 161 (2019) 386–397.

[56] I. Hossain, H.M. Rasel, M. Imteaz, F. Mekanik, Long-term seasonal rainfall forecasting using linear and non-linear modelling approaches: a case study for Western Australia, Meteorol. Atmos. Phys., 132 (2019) 131–141.

[57] Y. Lin, P.C. Lee, K.C. Ma, C.C. Chiu, A hybrid grey model to forecast the annual maximum daily rainfall, KSCE J. Civ. Eng., 23 (2019) 4933–4948.

[58] A.P. Ayodele, E.E. Precious, Seasonal rainfall prediction in Lagos, Nigeria using artificial neural network, Asian J. Res. Comput. Sci., 3 (2019) 1–10.

[59] N. Bensafi, M. Lazri, S. Ameur, Novel WkNN-based technique to improve instantaneous rainfall estimation over the north of Algeria using the multispectral MSG SEVIRI imagery, J. Atmos. Sol. Terr. Phys., 183 (2019) 110–119.

[60] S.H. Pour, A.K.A. Wahab, S. Shahid, Physical-empirical models for prediction of seasonal rainfall extremes of Peninsular Malaysia, Atmos. Res., 233 (2020), doi: 10.1016/j.atmosres.2019.104720.

[61] B.T. Pham, L.M. Le, T.T. Le, K.T. Bui, V.M. Le, H.B. Ly, I. Prakash, Development of advanced artificial intelligence models for daily rainfall prediction, Atmos. Res., 237 (2020), doi: 10.1016/j.atmosres.2020.104845.
[62] M. Ali, R. Prasad, Y. Xiang, Z.M. Yaseen, Complete ensemble empirical mode decomposition hybridized with random forest and kernel ridge regression model for monthly rainfall forecasts, J. Hydrol., 584 (2020), doi: 10.1016/j.jhydrol.2020.124647.
[63] H. Gökçekuş, Y. Kassem, J. Aljamal, Analysis of different combinations of meteorological parameters in predicting rainfall with an ANN approach: a case study in Morphou, Northern Cyprus, Desal. Water Treat., 177 (2020) 350–362.
[64] L. Diop, S. Samadianfard, A. Bodian, Z.M. Yaseen, M.A. Ghorbani, H. Salimi, Annual rainfall forecasting using hybrid artificial intelligence model: integration of multilayer perceptron with whale optimization algorithm, Water Resour. Manage., 34 (2020) 733–746.
[65] K.L. Chong, S.H. Lai, Y. Yao, A.N. Ahmed, W.Z. Jaafar, A. El-Shafie, Performance enhancement model for rainfall forecasting utilizing integrated wavelet-convolutional neural network, Water Resour. Manage., 34 (2020) 2371–2387.
[66] V. Nourani, S. Uzelaltinbulat, F. Sadikoglu, N. Behfar, Artificial intelligence based ensemble modeling for multi-station prediction of precipitation, Atmosphere, 10 (2019), doi: 10.3390/atmos10020080.
[67] D.J. Livingstone, Artificial Neural Networks, Methods in Molecular Biology™, Humana Press, New York, 2009.
[68] Y. Kassem, H. Çamur, E. Esenel, Adaptive neuro-fuzzy inference system (ANFIS) and response surface methodology (RSM) prediction of biodiesel dynamic viscosity at 313 K, Procedia Comput. Sci., 120 (2017) 521–528.
[69] J. Cho, J. Lee, Multiple linear regression models for predicting nonpoint-source pollutant discharge from a highland agricultural region, Water, 10 (2018) 1–17, doi: 10.3390/w10091156.
[70] G. Tegegne, D.K. Park, Y.O. Kim, Comparison of hydrological models for the assessment of water resources in a data-scarce region, the Upper Blue Nile River Basin, J. Hydrol. Reg. Stud., 14 (2017) 49–66.